DOI: 10.61782/fa.2025.0014

FORUM ACUSTICUM
EURONOISE 2025

A MATHEMATICAL MODEL BASED DIGITAL TWIN FOR GEARBOXES OPERATING AT VARIABLE SPEEDS

Shahis Hashim **Sitesh Kumar Mishra** **Piyush Shakya***

Engineering Asset Management Group, Indian Institute of Technology Madras, Chennai, India

ABSTRACT

The gearboxes are vital components of most drive trains. The operation of gearboxes in applications such as wind turbines and manufacturing tools is characterised by sudden changes in loads, which may lead to variations in operational speed. Hence, visualising system dynamics in varied conditions becomes vital to operation planning. The role of the digital twins in industrial applications has led to streamlined virtual learning of the system dynamics. Further, the mathematical model-based digital twin is faster in computation than its counterpart, the finite element model, thus meeting the demand for real-time system simulations. The study presents a digital twin based on a mathematical model for simulating the vibration response of a fixed-axis single-stage spur gearbox operating at variable speed. A detailed study of the simulated vibration response and a detailed discussion of its time, frequency, and time-frequency domains are also presented.

Keywords: *Dynamic model, vibration analysis, gearbox, digital twin*

1. INTRODUCTION

Lack of proper maintenance is the most prominent reason for gearbox failures [1]. Further, the failure of gearboxes may lead to extensive hazards ranging from operational downtime to loss of personal life [2]. Historically, gearbox failure has been the primary cause of aviation hazards. Notably, gearbox failures of the Boeing-made V-22 Osprey and the Airbus-made super-puma family helicopters have resulted in multiple fatal accidents over the years, with loss of life amounting to dozens [3]. Hence, visualising the gearbox's operation and the associated system dynamics is paramount for operation planning [4, 5]. The analyst may simulate varying operational conditions of the gearbox in a virtual system to understand the safe operational parameters. Such virtual visualisations are aided by a Digital twin (DT) capable of simulating the operational characteristics of the gearbox in a display unit.

A vast range of research addresses the DT analysis by Finite element modelling (FEM). However, the FEM is computationally intensive, requiring dedicated workstations and associated equipment. The FEM-based DTs are thus limited to industrial units that may afford such costly tools for operational optimisation. Most industrial units and primary employment providers in the developing and under-developed nations are categorised as micro, small, and medium enterprises (MSMEs). The non-availability of advanced algorithms for optimised operations significantly hinders developing nations' inclusive progress. As such, the dynamic model-based DTs that provide low-cost computation may be more suited to the context of MSMEs [6].

Researchers have tried to generate a dynamic model-based DT for gearboxes at various degrees of freedom [7]. Patel and Shakya demonstrated a model capable of addressing the variable speed but limited the study to signal processing of the simulated vibration response [8]. The present study explores the characteristics of the simulated vibration response during the presence of the fault, as well as during variations in speed, a vital aspect of the digital twin's onboard application.

*Corresponding author: pshakya@iitm.ac.in.

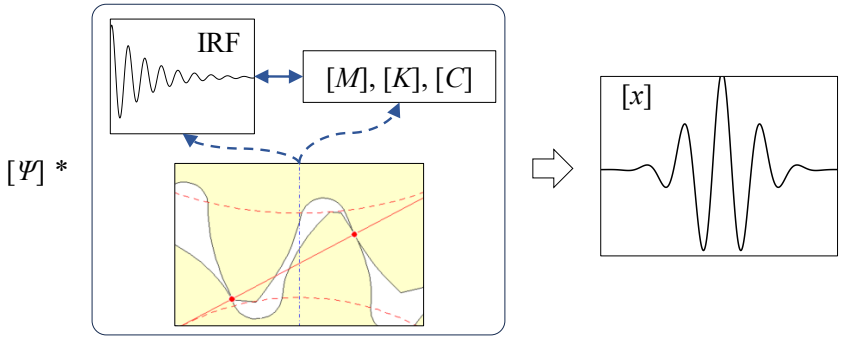

Figure 1: Schematic representation of vibration response during gear tooth meshing

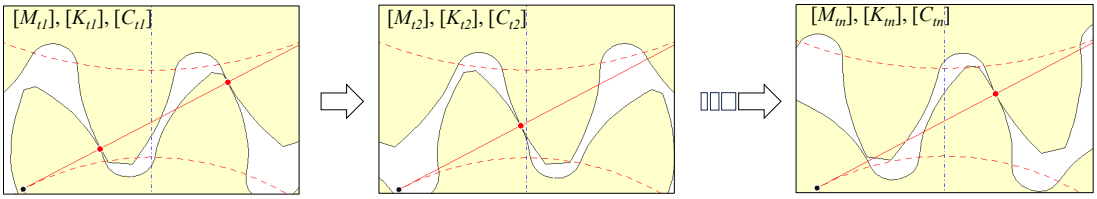

Figure 2: Gear mesh at different instants

2. VIBRATION RESPONSE SIMULATION

The vibration response-based analysis has emerged as the norm in contemporary gearbox monitoring practices. The wide acceptance of vibration analysis is due to its ability to reflect highly correlated fault information swiftly. The vibration response of a structural element is governed by its Impulse response function (IRF), which is dependent on the system's dynamic properties. The Figure 1 illustrates the instantaneous vibration response ($[x]$) generation during the gear tooth meshing under the influence of external and internal forces ($[\Psi]$). At any instant, the meshed gear tooth may be assumed as a structure with a set of dynamic properties dependent on the combined meshed geometry of the interacting gear tooth. The dynamic properties such as the mass ($[M]$), stiffness-coefficient ($[K]$), and damping-coefficient ($[C]$) influence the IRF of the said structure. However, the meshing of the gearbox generates complex meshed structures and dynamic forces at every instant, generating a complex vibration response over time (Figure 2). Nonetheless, understanding the vibration response is fundamental to the study. The following sections of the current study analyse the gearbox vibration response using the proposed dynamic model. The vibration response's time, frequency, and time-frequency domain characteristics are studied.

3. THE DYNAMIC MODEL

The dynamic property most influential in the vibration response generation is the instantaneous stiffness during the gear tooth meshing, termed the time-varying mesh stiffness (TVMS). The dynamic model consists of two integral parts: the TVMS calculation and the lumped-mass dynamic model. The root-crack growth under different speed variations is analysed in the present discussion to understand the complex nature of gearbox vibration response under fault growth and operational variations.

3.1 TVMS calculation

The dynamics of a single tooth during the gear mesh is assumed to be that of a cantilever beam under a moving load (Ψ). The Ψ results in a set of deformation modes of the gear tooth governed by the associated stiffness. Specifically, the gear tooth undergoes axial deformation, bending and shearing, fillet foundation deflection, and contact deformation. The present analysis adopts the Mohammed et. al. [9] model for the axial, bending, and shear stiffness (K_a, K_b, and K_s); Sainsot model [10] for fillet foundation stiffness (K_f); and Yang model [11] for the Hertzian contact stiffness (K_h).

The strain energies (U_a, U_b, and U_s) stored in the gear tooth due to the axial, bending, and shear deformation are

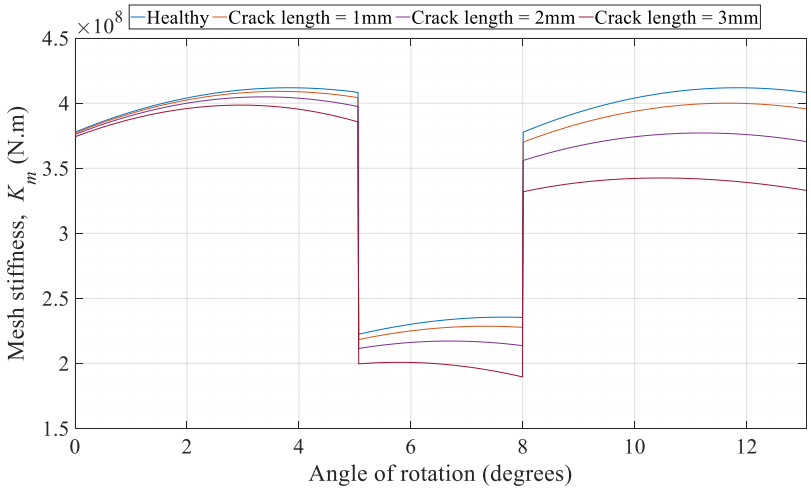

Figure 3: Calculated mesh stiffness for contact ratio of 1.5

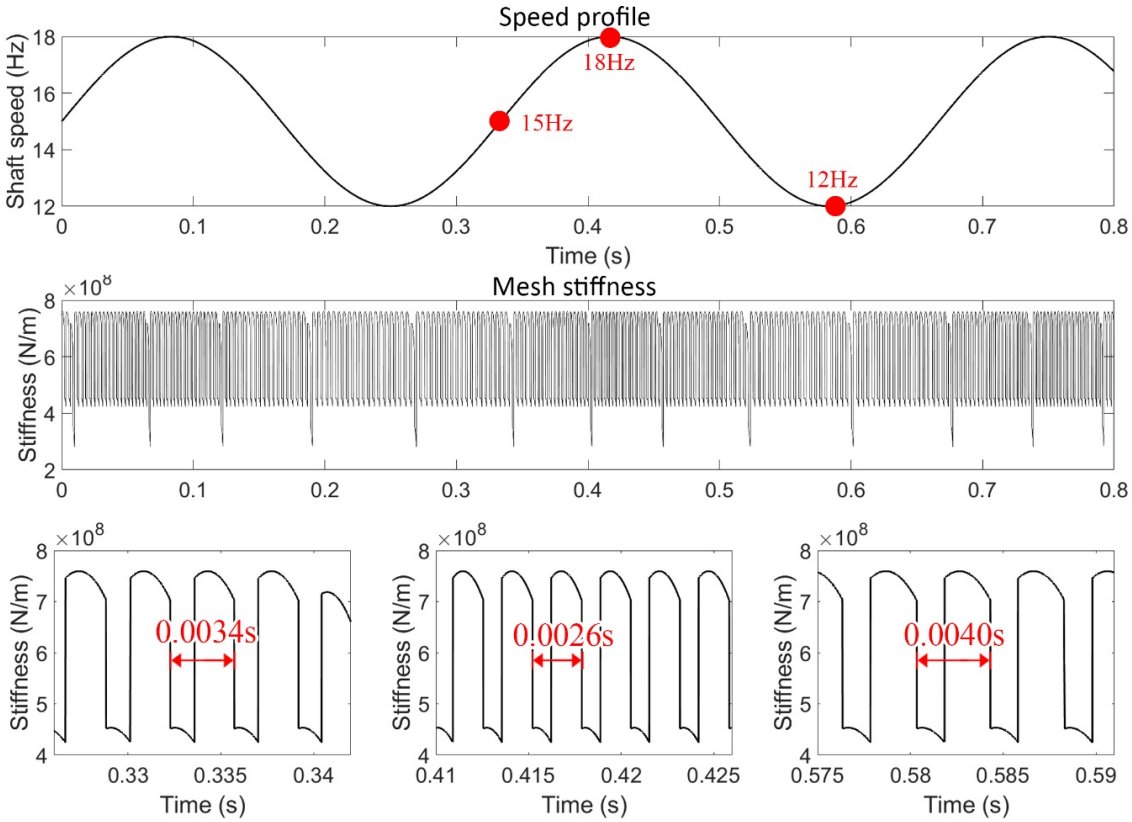

Figure 4: Instantaneous shaft speed and corresponding mesh stiffness of the gear operating at 15% speed fluctuation.

as follows:

$$U_a = \frac{\Psi^2}{2K_a} = \int_0^d \frac{\Psi_a^2}{2EA_X} dX \ , \Psi_a = \Psi \cos(\theta_1) \quad (1)$$

$$U_s = \frac{\Psi^2}{2K_s} = \int_0^d \frac{\Psi_b^2}{2EA_X} dX \ , \Psi_b = \Psi \sin(\theta_1) \quad (2)$$

$$U_b = \frac{\Psi^2}{2K_b} = \int_0^d \frac{J^2}{2EI_X} dX \ , \quad J = [\Psi_b.(d-X)] - [\Psi_a.h] \quad (3)$$

Here, the variables h, d, and X are associated with the gear tooth geometry and the point of contact. The E and G are the elastic and shear modulus. The I_X and A_X are the moments of inertia and cross-sectional area of the tooth section at a distance of X. The I_X and A_X are calculated as follows:

$$I_X = \begin{cases} \frac{1}{12}(h_X + h_X)^3 db; & h_x \leq H_o \\ \frac{1}{12}(h_X + H_o)^3 db; & h_x > H_o \end{cases} \quad (4)$$

$$A_X = \begin{cases} (h_X + h_X) db; & h_x \leq H_o \\ (h_X + H_o) db; & h_x > H_o \end{cases} \quad (5)$$

Here, H_o is the geometric parameter associated with the crack.

Further, the fillet foundation stiffness (K_f) and the Hertzian contact stiffness due to the Ψ is calculated by the following equation:

$$\frac{1}{K_f} = \frac{\cos^2(\alpha_1)}{bE} \left\{ L^* \left(\frac{d}{S_f}\right)^2 + M^* \left(\frac{d}{S_f}\right) + P^* \left(1 + Q^* \tan^2(\theta_1)\right) \right. \quad (6)$$

$$\frac{1}{K_h} = \frac{4(1-\nu^2)}{\pi E b} \quad (7)$$

Here b is the tooth width, and S_f is the tooth thickness at the fillet foundation. The $L*$, $M*$, $P*$, and $Q*$ are coefficients calculated empirically.

The total mesh stiffness (K_m) for the gear pair [1] at any instant is given by the following equation [2]:

$$\frac{1}{K_m} = \left(\frac{1}{K_{ag}} + \frac{1}{K_{bg}} + \frac{1}{K_{sg}} + \frac{1}{K_{fg}} + \frac{1}{K_{hg}}\right) + \left(\frac{1}{K_{ap}} + \frac{1}{K_{bp}} + \frac{1}{K_{sp}} + \frac{1}{K_{fp}} + \frac{1}{K_{hp}}\right) \quad (8)$$

[1] Note that the calculation shown here is for a single gear pair. Twice the value may be taken when multiple gear pairs are in mesh, i.e. when the contact ratio is more than one.

[2] The annotations p represents the pinion and g represents the gear.

The mesh stiffness for healthy and cracked gear tooth pair is simulated using the gear parameters given in [8] (Figure 3). It may be noted that the stiffness reduces with the increase in crack length. Also, at angular positions of multiple gear meshes, the K_m is higher due to the combined geometry. The period of engagement and disengagement of the gear tooth pair varies according to the instantaneous speed. The meshing is faster at higher speeds, while the meshing is slower at lower speeds. Hence, the mesh stiffness follows a scaling pattern driven by the speed of the instantaneous shaft. Figure 4 shows the speed profile, corresponding mesh stiffness and enhanced portions of the mesh stiffness time snippets. The scaling effect of the mesh stiffness across the time domain may be visualised by the period of engagement and disengagement at different speeds (15Hz, 18Hz and 12Hz).

3.2 Lumped mass model

A six-degree-of-freedom lumped mass model is used for the analysis [8]. Figure 5 shows a schematic representation of the model. A set of ordinary differential equations governs the dynamics of the said system. The equations of motion of the model are as follows:

$$I_g\ddot{\theta_g} = T_{fg} + r_g W_0 + T_g \quad (9)$$

$$I_p\ddot{\theta_p} = T_{fp} - r_p W_0 + T_p \quad (10)$$

$$m_g\ddot{v_g} + c_{gv}\dot{v_g} + k_{gv}v_g = -W_0 \quad (11)$$

$$m_p\ddot{v_p} + c_{pv}\dot{v_p} + k_{pv}v_p = W_0 \quad (12)$$

$$m_g\ddot{u_g} + c_{gu}\dot{u_g} + k_{gu}u_g = -\Psi \quad (13)$$

$$m_p\ddot{u_p} + c_{pu}\dot{u_p} + k_{pu}u_p = \Psi \quad (14)$$

$$W_0 = C_m(r_p\dot{\theta_p} - r_g\dot{\theta_g} + \dot{v_p} - \dot{v_g}) + K_m(r_p\theta_p - r_g\theta_g + v_p - v_g) \quad (15)$$

In the above-given equations, u, v, and θ represent the horizontal, vertical, and angular displacements; m is the mass, and r is the base radius; c and k represent the damping coefficient and stiffness of the gearbox bearings; T represents the input/output torque; T_f represents the frictional torque; K_m and C_m represent the mesh stiffness and the mesh damping coefficient respectively. The following paragraphs analyse the vibration response generated by the above-described dynamic model. Analyses based on time, frequency, and time-frequency domains are presented. Two cases of analyses are presented: Case 1, crack growth model and Case 2, speed variation model.

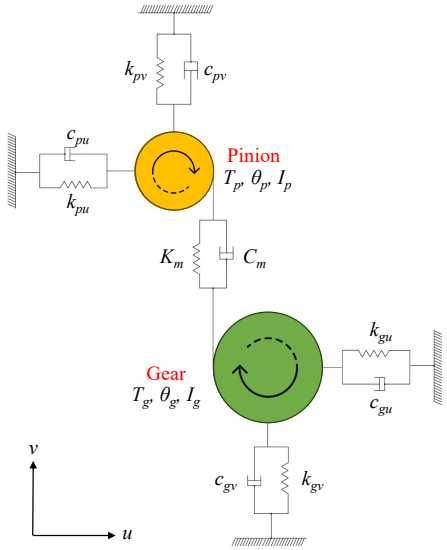

Figure 5: Six degree-of-freedom lumped mass model of a single-stage fixed-axis gearbox

The Case 1 is analysed using responses generated for K_m values given in the Figure 3. A sinusoidal variation with fluctuations 0%, 1%, 2.5%, and 5% are considered for Case 2.

4. RESULTS AND DISCUSSION

Analyses based on time, frequency, and time-frequency domains are presented in the following paragraphs. Two cases of analyses are presented: Case 1, crack growth model and Case 2, speed variation model. Case 1 is analysed using responses generated for K_m values in Figure 3. A sinusoidal variation (Figure 6) with fluctuations (F_l) 0%, 1%, 2.5%, and 5% are considered for Case 2.

4.1 Time domain analysis

The time domain representations of the vibration response generated for both cases are shown in Figures 7 and 8. The crack growth model shows the transient response in faulty gear mesh instances. Further, the transients correspond to the diminished stiffness of the meshed tooth pair, as shown in Figure 3. It may be noted that the damping of transient response after the impact of the faulty gear pair meshing has shown visible Amplitude Modulation (AM) (as shown in Figure 7). However, the direct visualisation of fault information from the time domain is impossible

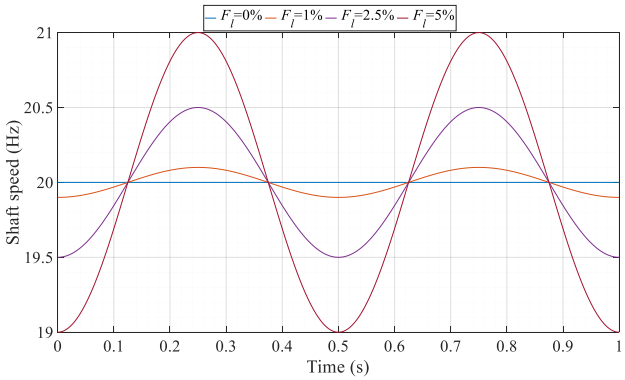

Figure 6: Speed variation for the simulation model

for very early faults. The said conundrum is multi-fold for real-life systems where external noise, sub-component vibrations, and transfer path effect mask the sensor-acquired vibration response. The variation in tooth contact force during the speed variation has resulted in a corresponding variation in the vibration response for Case 2 [3]. AM corresponding to the speed profile is apparent only in the vibration response corresponding to higher speed fluctuations. Intuitively, since the angular displacement is non-constant during the rotation of the gear pair, Frequency modulation (FM) is also expected in the response.

4.2 Frequency domain analysis

The frequency domain representation is a global illustration of the energy distributed among the constituent frequencies of the vibration response. The basis of the frequency domain representation is the Fourier transform. The Fourier transform facilitates any function to be represented as a combined set of scaled sinusoidal functions at different frequencies and phases. The Fourier transform of the vibration response ($x(t)$) is as follows:

$$\hat{x}(\omega) = \int_{-\infty}^{\infty} x(t) \mathrm{e}^{-i\omega t} dt \tag{16}$$

Theoretically, the gear pair meshes at constant operational speeds at a constant frequency, termed the Gear Mesh Frequency (GMF) [4]. Hence, the vibration responses will have a higher energy concentration at the GMF harmonics. Further, the gear tooth bends at every gear mesh. Hence, a

[3] The variation in shaft speed corresponds to variation in power transmission. Correspondingly, the torque load changes with respect to the speed variation.

[4] GMF is the fault frequency (f_0) for gearboxes.

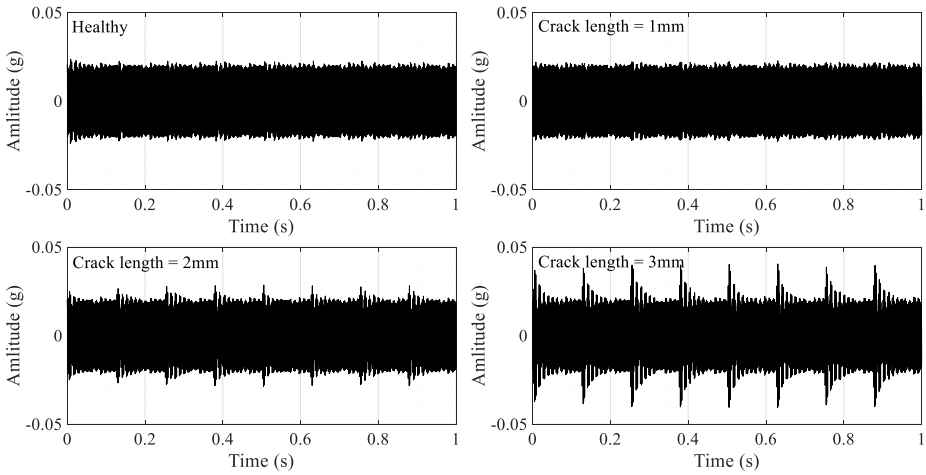

Figure 7: Time domain representation of the dynamic model simulated vibration response for different crack size

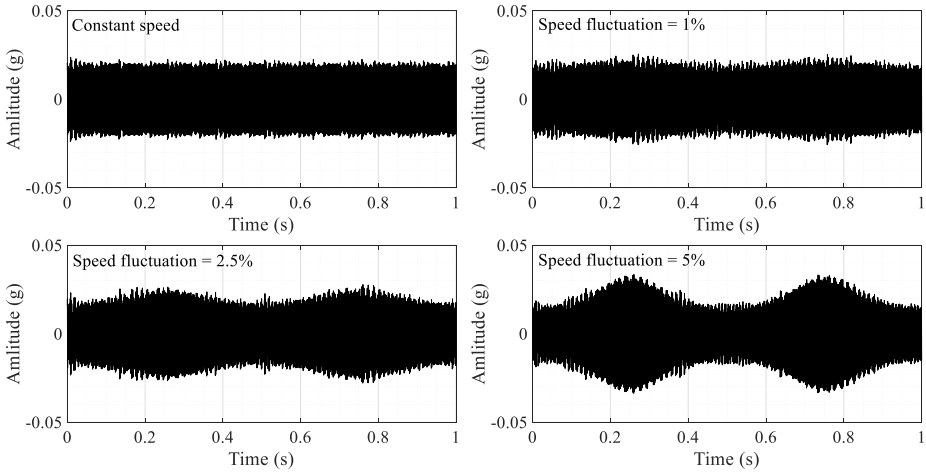

Figure 8: Time domain representation of the dynamic model simulated vibration response for different speed fluctuation

slight variation in transmission ratio at the tooth meshes leads to FM, which, along with the AM due to gear mesh impacts, leads to sidebands around the GMF. Further, the AM-FM at the faulty gear pair mesh is higher than the rest due to the relatively lower K_m. Hence, the presence of the fault leads to disturbance in the sideband energy, which is apparent in the frequency domain representation of the crack growth model's vibration response (Figure 9a). The basic assumption of frequency domain representation is the constant operational speed. As such, the frequency domain representation of the vibration response of gearboxes operating at variable speeds results in a smeared spectrum (Figure 9b). Specifically, the global GMF variation across the gearbox's operation varies; hence, the vibration response energy gets smeared across those frequencies. Further, a decrease in the spectral amplitude is also apparent, possibly due to the smearing of energy across the earlier frequencies concentrated at singular frequency values [5] .

[5] Note that the total vibration energy stays conserved.

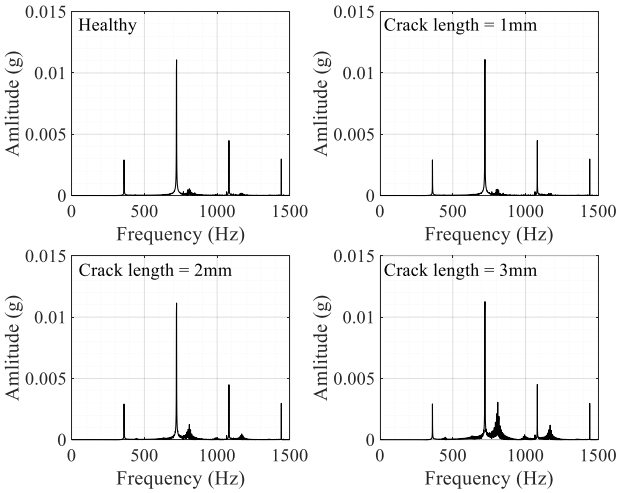

(a) Frequency domain representation of the dynamic model simulated vibration response for different crack sizes.

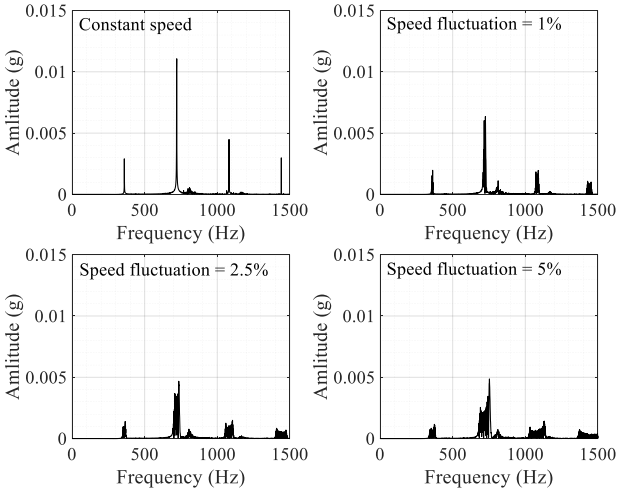

(b) Frequency domain representation of the dynamic model simulated vibration response for different speed fluctuations.

Figure 9: Frequency domain representations of simulated vibration responses for different conditions.

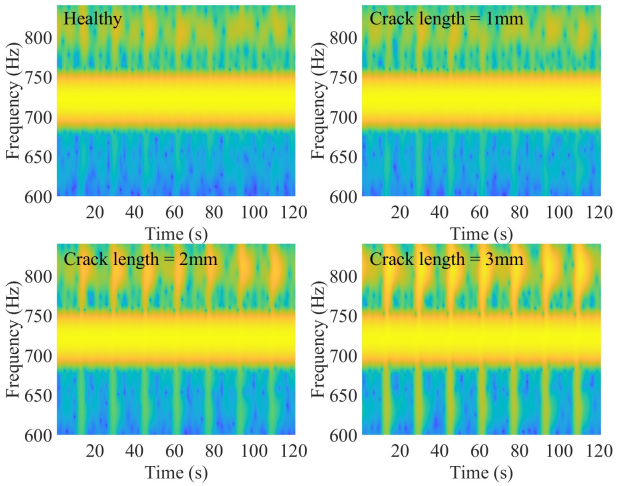

(a) Time-frequency domain representation of the dynamic model simulated vibration response for different crack sizes.

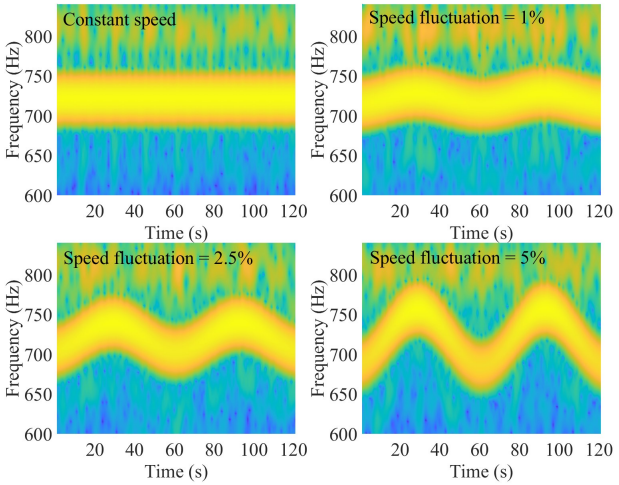

(b) Time-frequency domain representation of the dynamic model simulated vibration response for different speed fluctuations.

Figure 10: Time-frequency domain representations of simulated vibration responses for different conditions.

4.3 Time-frequency domain analysis

In contrast to the frequency domain representation, a global representation of vibration response energy across the frequencies, the time-frequency domain representation illustrates a temporal localised frequency distribution. The time-frequency domain is the frequency domain amalgamation of time-windowed signal sections of the vibration response.

$$\hat{x}(\tau,\omega) = \int_{-\infty}^{\infty} x(t)w(t-\tau)\mathrm{e}^{-i\omega t}dt \qquad (17)$$

Here, $w(.)$ represents the windowing function. The time-frequency domain representation provides insights into the localised variation in frequencies. Specifically, the

frequency variations, which are difficult to capture by the frequency domain analysis due to spectral smearing, are easily comprehensible in the time-frequency domain representation.

Figures 10a and 10b show the time-frequency domain representations of vibration responses generated for the crack growth and speed variation models. The variations in instantaneous frequency are apparent in both cases [6]. Specifically, the crack growth model was simulated at a constant speed; hence, the GMF stays constant over time. However, in the speed variation model, the time-frequency representation aptly illustrates the variations in GMF due to shaft frequency fluctuation. In the crack growth model, frequency variations may be observed at the fault transients due to their FM nature. The time-frequency representation provides clear insight into the frequency variation of the vibration response across time. However, the spectral coherence of the representation is limited by the time and frequency resolution balance across the respective axes [7]. Hence, spectral energy quantification for fault severity estimations is not easily possible in the time-frequency domain. When combined with appropriate fault enhancement algorithms, the frequency domain analysis has shown better quantification of fault severity. Nonetheless, the time-frequency representation is ideal for reverse estimation of instantaneous frequency in the unavailability of tacho-pulse signals.

5. CONCLUSION

The study presents a digital twin based on a dynamic model for simulating gearbox vibration response in the presence of a fault and variable operational speed. The six-degree-of-freedom model successfully simulates the vibration response characteristic of a gearbox with root cracks and operates at variable speed. Further, a detailed study of the vibration response in its time-domain, frequency-domain, and time-frequency domain is presented. The presented model can simulate the vibration response's spectral distortions and amplitude-frequency modulations indicative of fault information and speed variations.

[6] The second GMF harmonic is shown in the figures due to its higher spectral energy concentration, as apparent in the frequency domain representations.

[7] Heisenberg's uncertainty principle.

6. REFERENCES

[1] J. R. Davis, *Gear materials, properties, and manufacture*. ASM international, 2005.

[2] S. Hashim and P. Shakya, "Tacho-less spur gear condition monitoring at variable speed operation using the adaptive application of variational mode extraction," *Structural Health Monitoring*, 2024.

[3] L. Zhou, F. Duan, M. Corsar, F. Elasha, and D. Mba, "A study on helicopter main gearbox planetary bearing fault diagnosis," *Applied Acoustics*, vol. 147, pp. 4–14, 2019.

[4] S. Hashim and P. Shakya, "Variational mode decomposition based vibro-acoustic analysis for spur gear fault detection," in *Internoise and Noisecon Congress and Conference Proceedings*, pp. 1995–2994, Institute of Noise Control Engineering, 2023.

[5] S. Hashim, S. K. Mishra, and P. Shakya, "An approach for adaptive filtering with reinforcement learning for multi-sensor fusion in condition monitoring of gearboxes," *Computers in Industry*, vol. 164, p. 104214, 2025.

[6] G. Sariyer, S. Mangla, Y. Kazancoglu, C. O. Tasar, and S. Luthra, "Data analytics for quality management in industry 4.0 from a msme perspective," *Annals of Operations Research*, 2021.

[7] X. Liang, M. Zuo, and Z. Feng, "Dynamic modeling of gearbox faults: A review," *Mechanical Systems and Signal Processing*, vol. 98, pp. 852–876, 2018.

[8] A. Patel and P. Shakya, "Spur gear crack modelling and analysis under variable speed conditions using variational mode decomposition," *Mechanism and Machine Theory*, vol. 164, 2021.

[9] O. Mohammed and M. Rantatalo, "Gear fault models and dynamics-based modelling for gear fault detection – a review," *Engineering Failure Analysis*, vol. 117, 2020.

[10] P. Sainsot, P. Velex, and O. Duverger, "Contribution of gear body to tooth deflections—a new bidimensional analytical formula," *J. Mech. Des.*, vol. 126, no. 4, pp. 748–752, 2004.

[11] D. Yang and Z. Sun, "A rotary iodel for spur gear dynamics," *Journal of Mechanical Design, Transactions of the ASME*, vol. 107, no. 4, p. 529 – 535, 1985.